Investigations in Superconductivity

Lulu Liu (Partner: Chris Chronopoulos)
MIT Undergraduate
(Dated: May 15, 2008)

We confirm key properties associated with the phenomenon of superconductivity. Among these are the zero resistivity of the superconducting material, the Meissner effect, the temperature dependence of the critical external magnetic field (B_c), the existence of persistent currents, the band gap and the Josephson current. Transition temperatures (T_c) are measured for several Type I superconductors– found to be 5.42 ± 0.06 K for vanadium, 6.8 ± 2.3 for lead, and 9.4 ± 0.1 K for niobium. Investigations into high T_c superconductor YBCo yielded a T_c of 135 ± 30 K, and a linear frequency dependent AC impedance of the superconductor at frequencies over 1000 kHz. We observe Josephson and Giaever tunneling and calculate from our results a value for the flux quantum, $\Phi = (1.6 \pm 0.1) \times 10^{-7}$ G cm^2.

1. INTRODUCTION

A perfect conductor is an idealized material of zero resistivity. These materials, when placed in a varying external magnetic field, can be found to obey the following relation [2] for the magnetic field at depth z,

$$\dot{\vec{B}}(z) = \dot{\vec{B}}(0)e^{-\frac{z}{\lambda}} \quad (1)$$

That is to say, beyond a certain characteristic depth, λ, the magnetic field flux is frozen in its constant, initial state. The requirement for superconductivity is more stringent. Superconductors not only exhibit zero resistivity, but also have been discovered to expel all magnetic flux from the interior of the material. This is known as the Meissner effect, and can be summarized in the equation (derived by F. and H. London) [1],

$$\vec{B}(z) = \vec{B}(0)e^{-\frac{z}{\lambda_L}} \quad (2)$$

which states, that a magnetic field may penetrate a superconductor only to a depth comparable to λ_L, termed the London penetration depth, beyond which the magnetic field is uniformly zero. The mechanisms responsible for these and other remarkable phenomena of superconductivity remained a mystery for many years after its initial discovery. That is, until the advancement of the BCS theory of superconductivity in 1957 [3].

2. OVERVIEW OF BCS THEORY

The BCS theory relies on the notion of a small energetic perturbation due to the interaction of electrons with the vibrational modes, or phonons, of the solid lattice of ions in which they are free to move. This interaction generates an effective attraction between remote electrons. The phonons act as a third party, using individual electron attraction to the ion lattice to facilitate mutual attraction between electrons. This effect is generally negligible except under conditions of very low temperatures, in which case the interaction becomes dominant over Coulomb repulsion and leads to remote electron-electron coupling. The requirement for the creation of these electron pairs, called Cooper pairs, is that the thermal energy (kT) in the environment be less than the binding energy holding the pairs together. The temperature at which this occurs is called the critical temperature, T_c.

The significance of these Cooper pairs becomes at once evident upon examination of their behavior. Single electrons with spin-1/2 behave as fermions, their allowed states governed by the Pauli Exclusion Principle which allows no two fermions to occupy the same quantum state. This leads to a filling of higher and higher energy levels by individual electrons within a material, resulting in an energy spectrum that is dense and quite broadly ranged. Normal resistivity is caused by momentum loss in the charge carriers through excitation interactions with the environment. Densely spaced states and the abundance of available energy in the system makes this a frequent occurrence. On the other hand, the combined spin of two electrons is an integer. This implies that the wavefunctions of Cooper pairs are symmetric, and that Cooper pairs are actually bosons, which not only are not subject to the Pauli Exclusion Principle, but in fact have an affinity to occupy the same state as other bosons in a system. At temperatures below the critical temperature, all Cooper pairs have essentially condensed into a single ground state, and a great amount of energy is required to excite any bosons into a higher state. This energy gap is much greater than the average energy of the system so this interaction is extremely rare. The charge carriers flow on uniformly and unobstructed, leading to a material's zero resistivity.

T_c can now be considered a phase transition temperature for the superconductor. At a temperature $T > T_c$, thermal energy is enough to break apart the Cooper pairs and return the material to a normally conducting (NC) state. Analogously, the presence of an external magnetic field, if it is large enough, can also induce an NC transition. The minimum magnitude of the external field necessary to quench a particular superconductor is called the critical field, B_c. This quantity is strongly correlated with the critical temperature and the band gap, and depends quadratically on the temperature, T.

$$B_c(T) = B_0 \left[1 - \left(\frac{T}{T_c} \right)^2 \right] \tag{3}$$

We wish to experimentally verify the existence and the various theoretical implications of superconductivity, beginning with a well-defined zero-field transition temperature and the Meissner effect.

3. MEISSNER EFFECT AND THE T_c OF VANADIUM

Two nested solenoids surrounding a superconducting material are mounted on the end of a long probe to be inserted into a dewar containing liquid Helium at 4.2K. Temperature is tracked by measuring voltage drop across a calibrated silicon diode with reference to the manufacturer's spec sheets [5], and controlled by regulating helium flow. Naturally, an AC current applied to one solenoid would induce an EMF in the other,

$$EMF = -N\frac{d\Phi}{dt} \tag{4}$$

where N is the number of turns of the test coil and Φ is the total magnetic flux through its center. We expect to see a sudden drop in EMF as the material transitions into its superconducting phase due to the reduction in total magnetic flux. We do not expect the EMF to disappear entirely since the superconducting material will not completely fill the enclosed space. Waveforms are monitored on an oscilloscope for the moment of transition and the corresponding temperature recorded.

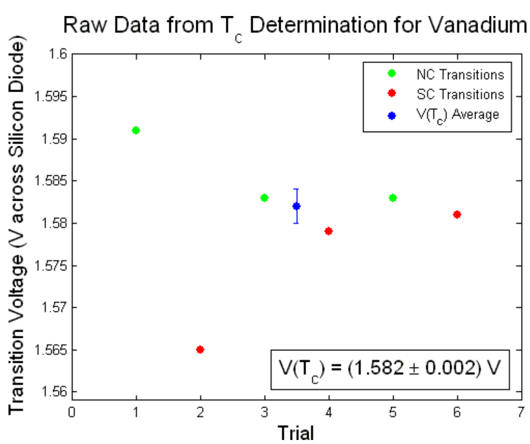

FIG. 1: The hysteresis effect was observed during our measurement of the T_c of vanadium.

Indeed, we do observe an amplitude drop from 27.1 mV to 19.3 mV in EMF at the SC transition for vanadium. Figure 1 shows the six T_c values obtained consecutively by alternately varying the temperature. Three NC transitions and three SC transitions were recorded. The *hysteresis* effect is evident here, observed as a lag between the environmental input (in this case, a change in temperature) and the system's response. The magnitude of the hysteresis effect increases with increased load on the system. This means a faster rate of change of temperature would cause a greater lag in system transition.

For this reason the first two data points are excluded from the final determination of T_c as they were taken before the temperature stabilized. We find for vanadium a T_c of 5.42 ± 0.06 K, which agrees well with the established T_c of 5.4 K [7]. It was at this point in our investigation (after the first lab day) that Probe I was taken out of commission. We turn to the setup in Probe II and the investigations in persistent current and critical field curve for lead.

4. SUPERCONDUCTING LEAD

4.1. Equipment and Calibration

At the end of this probe a 44.5 mm long solenoid with 2210 turns is wound around a hollow lead cylinder. Mounted on the interior of this cylinder is a hall probe, to measure the enclosed magnetic field, and a carbon resistance thermometer (CRT) for a rough temperature determination. Though the CRT's resistance decreases monotonically with increasing temperature, it obeys no simple relation over a large range of temperatures. We are forced to use the closest analytical expression determined empirically [6] for such a resistor,

$$\mathrm{Ln}R + \frac{C}{\mathrm{Ln}R} = A + \frac{B}{T} \tag{5}$$

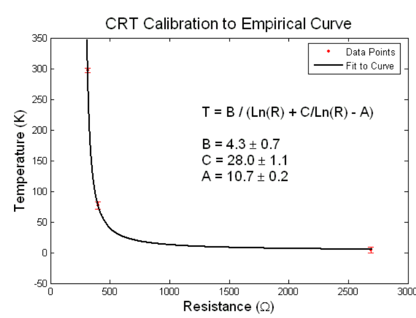

FIG. 2: Three parameter calibration of the carbon resistance thermometer.

Available (R,T) data points for our calibration were liquid helium (4.2K), liquid nitrogen (77K), and room temperature (297.6K). The best fit curve to those three points is pictured in Figure 2. Due to the sensitivity of the T vs. R relation in the low and high T region, and the uncertainty of the data points themselves (see 7 on Errors), the accuracy of this curve is somewhat suspect.

Uncertainty generated in the initial calibration will propagate to all calibrated measurements and results.

In addition, the conversion from measured Hall voltage to magnetic field strength in units of Gauss was also done via a calibration, though in this case, a linear one. The curve itself is not pictured.

4.2. Persistent Current

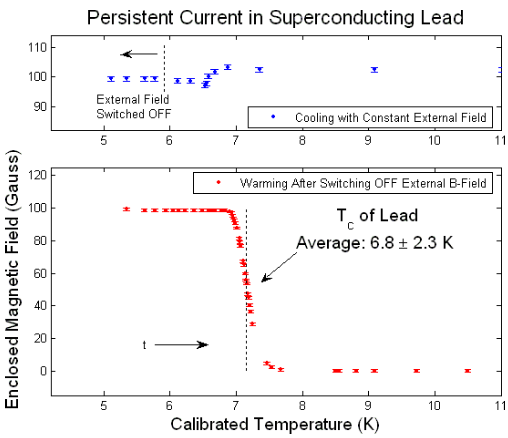

FIG. 3: Arrows indicate the direction of increasing time on this figure. In the upper graph a small kink in the expected flat behavior occurs as the material enters superconducting state due to the imperfect geometry (finite lengths, etc) of the cylinder and solenoid. This small deviation, along with the rapid dissipation of the persistent current at the NC transition, bound the value of the actual critical temperature.

We generate a persistent current in lead following a simple procedure. While the sample is in its normally conducting state, the outer solenoid is fed a steady DC current which generates a constant magnetic field oriented along the axis of the cylinder. The sample is then brought through its superconducting transition, at which point two oppositely flowing currents turn on near the inner and outer surfaces of the hollow lead cylinder and work to generate a field that exactly cancels the external field within the material. Ideally, we should see no change in the enclosed field if the cylinder and solenoid were infinitely long. Then, the external field is turned off. The outer current ceases, but the inner current persists, resistant to change in enclosed flux. Readings from the hall probe should indicate no change, as the flux has been frozen in. After some time, the superconductor is then warmed up gradually. We look for the dissipation of the persistent current as the material exits its superconducting phase. For our results please see Figure 3.

The hysteresis effect should be comparable in both directions, and can be removed by an average of the two transition temperatures. We obtain, for the critical temperature T_c of lead, 6.8 ± 2.3 K. The accepted value is 7.2 K [7], within our (large) error bounds.

4.3. Critical Field Curve

Using the same equipment, but in this case, holding the temperature constant at a value $T < T_c$ whilst increasing the external field from zero, we are able to determine for that temperature the corresponding critical field value, $B_c(T)$. Figure 4 shows an example curve.

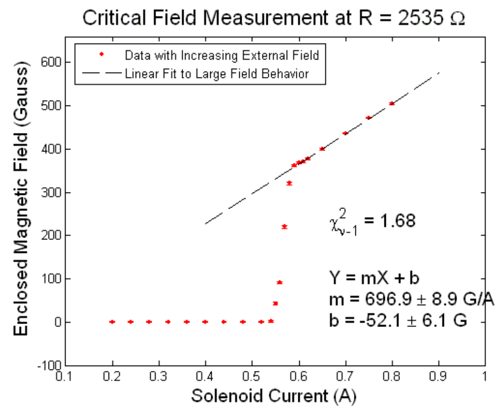

FIG. 4: Taken at a constant temperature (less than T_c) corresponding to a CRT resistance of 2535 Ω. Care is taken so that no flux is trapped during the initial SC transition. When the external field is turned on, currents are generated within the superconductor to resist a change in enclosed flux. At B_c, the superconductivity quenches, and we are left with the linear behavior one would expect of a normal conductor.

In order to verify that beyond the critical field, the material behaves as a normal conductor, we compare the fitted slope of the curve at high B-fields with the expected value for a material with a magnetic permeability of approximately 1. The measurement of enclosed magnetic field should reflect almost exactly the magnetic field generated by the solenoid.

$$B = \frac{\mu N}{L} I \tag{6}$$

and with $\mu \approx \mu_0$, $N = 2210$, and $L = 44.5mm$, we find that the slope of the B vs. I curve should be 624 G/A. The 696.9 G/A value obtained is in reasonable agreement considering the finite geometry.

Reiterating this procedure, alternately transitioning out of and into the superconducting state (the SC transition point identified by the sudden halting of linear response from the system indicative of frozen flux), we obtain critical field values for various resistance readouts. Conversion of the x-axis into temperature using the calibration given in 4.1, we produce the graph below, fit to the theoretical quadratic relation (Figure 5).

Given the large degree of uncertainty in our calibration, it's quite fortunate that we were able to recover with reasonable accuracy the critical temperature intersect from the best fit curve (7.5 ± 0.2 K in this case). We are not so lucky with the zero-Kelvin asymptotic critical field value, which the fit indicates should be approxi-

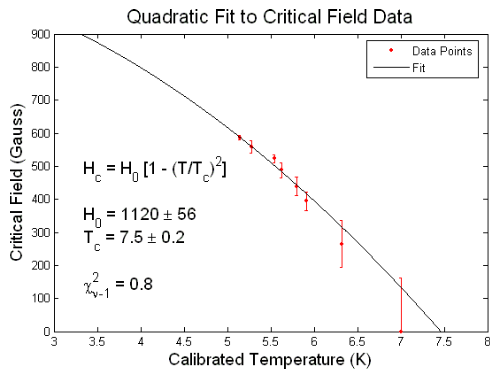

FIG. 5: Critical field curve for superconducting lead. The error bars are large due to calibration uncertainties.

mately 1100 Gauss, while the accepted upper critical field for lead is only 803 Gauss [8].

5. JOSEPHSON JUNCTION

5.1. Theory

Two conductors separated by a thin insulating barrier can nevertheless exchange electrons. The mechanism responsible is quantum tunneling of individual electrons, resulting in current. Since fermions can only tunnel into unoccupied states, the tunneling probability is proportional to the voltage difference for low bias (eV ¡¡ barrier height, ϕ) resulting in an ohmic I-V curve. When the conductors are superconductors, electrons near the Fermi level have all condensed into Cooper pairs, opening up an energy gap. A threshold voltage then arises (Giaever, [10]) for current flow, with energy at least equal to the energy necessary to excite an electron in a Cooper pair into the single particle conduction band, $eV_{min} = 2\Delta$ where Δ here is defined as the superconductivity energy gap, and 2Δ is the binding energy of the Cooper pair. Below this threshold we expect to see little to no current, and beyond this threshold an ohmic relation. From the BCS theory of superconductivity [3], Δ is related to T as follows,

$$\Delta(T) = 1.76kT_c\sqrt{1 - \frac{T}{T_c}} \tag{7}$$

However, Giaever-type tunneling is not the only mechanism by which current flows across a Josephson junction. Due to the bosonic nature of Cooper pairs, their tunneling, unlike that of a single electron, is not limited by available states. Assuming a single energy state for both sides of the junction and a couping between their wavefunctions, ψ_1 and ψ_2, we can derive the Josephson current expected to flow across the junction. Here, we substitute,

$$\psi_1 = \sqrt{\rho_1}e^{i\theta_1} \qquad \psi_2 = \sqrt{\rho_2}e^{i\theta_2} \tag{8}$$

with phase factors θ_1 and θ_2 and the difference between them $\delta = \theta_2 - \theta_1$ into a set of coupled Schrödinger Equations. We quote the results from Feynman [4].

$$J = \dot{\rho_1} = J_0 \sin\delta \tag{9}$$

$$\delta(t) = \delta_0 + \frac{q}{\hbar}\int V(t)dt \tag{10}$$

Their implications are quite unusual. It is immediately clear that with any finite DC voltage across the junction, the current flow from Cooper pairs oscillates very rapidly (frequency of order $q/\hbar$) and the net current is zero. On the other hand, if *no* voltage is applied, δ is a constant, and we should be able to observe a constant current of value ranging from J_0 to $-J_0$ flowing across the junction. This is known as the Josephson current, the effect of which is superimposed with the effects of Giaever tunneling.

5.2. Setup and Data

The junction is made of two orthongal, overlapping strips of niobium separated by an oxide layer 1.75 nm thick. We apply a low frequency oscillating bias across the junction and plot the current as a function of voltage on an oscilloscope. Josephson current data for four different temperatures is shown in Figure 6.

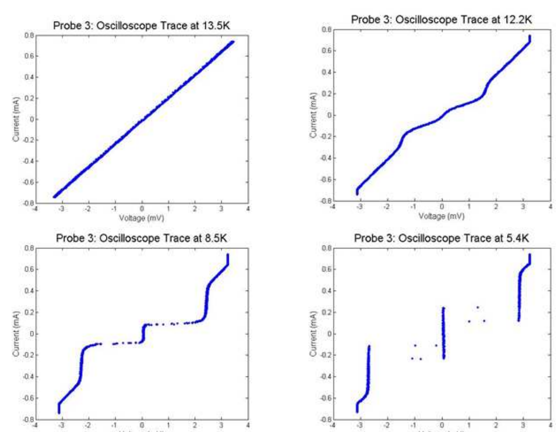

FIG. 6: Josephson junction current vs. voltage bias graphs. The material is a normal conductor in the top left graph. $V(T)$ is measured across the x-axis and $I(B)$ (see equation 20) across y.

Plotting our data for $\Delta = eV(T)$ against the temperature, we obtain the graph in Figure 7. The bet fit yields a T_c for niobium of 9.4 ± 0.1 K. The established value is 9.2 K.

5.3. Theory of the Flux Quantum

Consider a superconducting ring with a surface current generating an enclosed flux Φ. The wavefunction of the

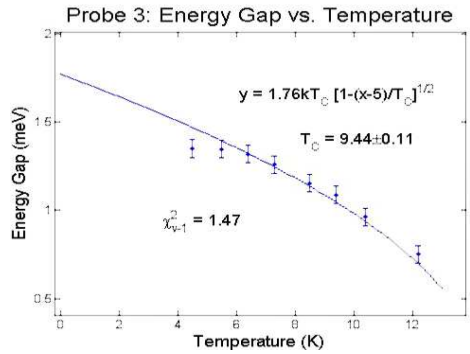

FIG. 7: Best fit to energy gap data. Wary of intrumental bias, a constant temperature offset was introduced.

cooper pairs can again be expresed as,

$$\psi(\vec{r}) = \sqrt{\rho(\vec{r})}e^{i\theta(\vec{r})} \tag{11}$$

the current density $\vec{J}$, is then [4],

$$\vec{J} = \frac{\hbar}{m}\left(\nabla\theta - \frac{q}{\hbar}\vec{A}\right)\rho \tag{12}$$

with $\vec{A}$ as the vector potential. Supercurrents flow at the very surface of superconductors. At a depth $\lambda >> \lambda_L$, the current density $\vec{J}$ is zero, and Equation 12 becomes,

$$\hbar\nabla\theta = q\vec{A} \tag{13}$$

taking a closed integral around the loop and using the relation $\oint \vec{A}\cdot ds = \Phi$,

$$\hbar\oint\nabla\theta\cdot ds = q\oint\vec{A}\cdot ds \tag{14}$$

$$\oint\nabla\theta\cdot ds = \frac{q}{\hbar}\Phi \tag{15}$$

We know that,

$$\int_a^b \nabla f\cdot ds = f(b) - f(a) \tag{16}$$

and we require only that the wavefunction be single valued, that $\psi(\theta(\vec{r_2})) = \psi(\theta(\vec{r_1}))$ if $\vec{r_1} = \vec{r_2}$, this, along with equation 16, leads to the contraint that $\oint\nabla\theta\cdot ds = 2\pi n$. We've derived the result that the enclosed flux Φ must be quantized with,

$$\Phi = \frac{nh}{q} = n\Phi_0 \tag{17}$$

where Φ_0 is the flux quantum, $h/2e$ with $q = 2e$ inserted for the Cooper pairs.

5.4. Magnetic Field Effects and the Flux Quantum

We apply a magnetic field in the plane of the oxide layer (say, along the y axis) perpendicular to the direction of Josephson current flow (in the z-direction). Inserting the relation $\nabla\times A = B$ into Equation 12, we can solve for the spatial dependence in the x direction of the phase difference $\delta(x) = \theta_2(x) - \theta_1(x)$, consequently the Josephson current as a function of x [12].

$$\delta = \frac{B_y}{\Phi_0}xt + \delta_0 \tag{18}$$

$$J_z = J_0\sin\left(\frac{B_y}{\Phi_0}xt + \delta_0\right) \tag{19}$$

The total current is then a function of the magnetic field and identical to the single slit diffraction of light.

$$I(B) = I(0)\left|\frac{\sin\pi(\Phi_B/\Phi_0)}{\pi(\Phi_B/\Phi_0)}\right| \tag{20}$$

where $I(0)$ is the maximum current at zero magnetic field, and $\Phi_B = B_yL(2\lambda_L + d)$ is the flux of the magnetic field through the junction with width along x of L and barrier thickness d in the z direction. Zeros of this function occur at $B_y = \frac{n\Phi_0}{L(2\lambda+d)}$. The flux quantum is calculated from the difference in field, ΔB_y, for two successive current minima,

$$\Phi_0 = \Delta B_yL(2\lambda_L + d) \tag{21}$$

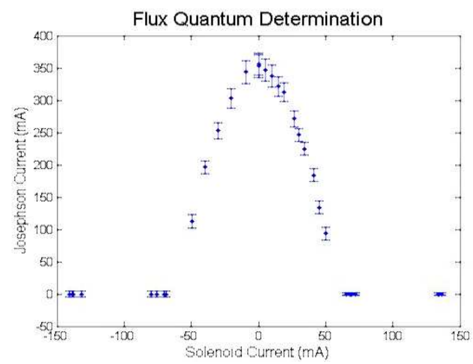

FIG. 8: Josephson current plotted against magnetic field strength, for measurement of the flux quantum.

Our data from the Josephson current measurement is shown in Figure 8. From these results we obtain for the flux quantum $\Phi_0 = (1.6\pm0.1)\times10^{-7}$G cm^2. Lower than the accepted value of 2×10^{-7} G cm^2. This could be due to a underestimate of the error or incorrect dimensions.

6. HIGH T_c SUPERCONDUCTORS

We've seen by now some of the remarkable properties exhibited by superconductors. Among the most alluring of its prospects yet out of our reach is the promise of lossless electrical transmission. Its benefits are obvious but unattainable with simple Type I superconductors. Their critical temperatures and critical field values are too low for economical everyday use.

Recently, due to the advent of high T_c superconductors, we've seen renewed interest in lossless transmission.

For the rest of the paper, we shall investigate some key properties of these Type II superconductors as a shallow look into the immediate plausibility of these materials in achieving this goal.

We verify YBCo as a high T_c superconductor. A strip of YBCo coated with silver is connected at its ends to a current source. The cooling agent is a small dewar of liquid nitrogen at 77K. We measure the voltage drop across the superconductor as a function of temperature as the material warms rapidly after removal from the dewar. At a temperature of 77K, the resistance of the material is indeed zero, indicating perfect conductivity. After transition out of the superconducting phase, the material's resistance is seen to increase linearly with temperature. Poor temperature control only allows an estimate of the NC transition temperature, which we find to be 135 $\pm$ 30 K, a value higher than the established T_c of 92 K [9].

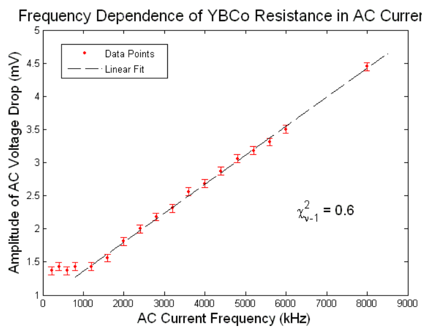

FIG. 9: Baseline of 1.4 mV noise. YBCo in its superconducting state (77K) has nonzero impedance for high frequency AC currents.

We note a peculiar behavior of YBCo superconductors when subject to an AC current, see Figure 9. At frequencies below 1000 kHz, the material exhibits zero impedance as expected. However, increasing the frequency further one observes a linear increase in impedance as a function of frequency.

This particular effect is quite damaging as high voltage transmission lines rely on AC current for propagation over very long distances. Clearly, lossless transmission is not easily achievable and there is still much work to be done.

7. ERRORS

For our work with the critical temperatures and fields of superconductors, a great majority of the uncertainty in our experiment came from the measurement and the control of the temperature. During our measurement of the critical field, while increasing and decreasing the current through the field-generating solenoid, we would often see fluctuations of 50-100 Ω in the carbon resistor. We did not have fine enough control over the flow to adjust for these deviations; instead, an average was taken between the initial resistance and the final resistance after each trial.

Poor temperature control also leads to mored marked hysteresis lags. If symmetric trials could be done with NC and SC transitions, they were, and the hysteresis effect removed by average. Sometimes this was not an option, such as was the case in the high T_c experiment, where in addition to there being present the systematic effect, the methodology also ensured its magnitude would be large, due to the rapid warming of the superconductor and surroundings.

Calibration of the thermometer became central to our work with Probe 2. With the highly sensitive and non-linear three-parameter/three-point calibration curve for the CRT, large uncertainties from calibration were propagated throughout the experiment. In the future, more calibration points would need to be obtained or a more accurate thermometer substituted.

Josephson data obtained on the oscilloscope were subject to the limitations of the scope. Too slow sampling rate of the oscilloscope resulted in somewhat misleading data in the region $|V| < 2\Delta/e$ where the average current is zero, we instead seem to see a steady positive and negative current. We believe this is due to the oscilloscope's tendency to extrapolate, and those points should be ignored.

8. CONCLUSIONS

We confirm the existence of superconductors distinct from perfect conductors. We observe properties unique to this material, including the Meissner effect, persistent currents, and quantization of magnetic flux. The T_c values we obtained for four superconductors is given in the table above. The critical field was measured against the temperature and fit to the predictions of the BCS theory with good agreement. As for the Josephson junction, our results were in line with what one would expect from a combination of both Giaever-type and Josephson-type tunneling both in terms of energy gap behavior and zero-voltage current as a function of magnetic flux. We obtain a value for the flux quantum Φ_0 of (1.6 $\pm$ 0.1) $\times 10^{-7}$ G cm^2.

Material	$T_c(K)$	Accepted Values (K) [7]
V	5.42 $\pm$ 0.06	5.4
Pb	6.8 $\pm$ 2.3	7.2
Nb	9.4 $\pm$ .1	9.2
YBCo	135 $\pm$ 30	92

Finally, we explored some of the properties of high T_c superconductors, including a linear R vs. T relation at low $T > T_c$ and a non-zero impedance for high frequencies even in its superconducting state. This particular peculiarity and others may have a heavy impact on the role of high T_c superconductors in the ongoing application of superconductors to cutting edge energy transport and technology.

[1] F. London and H. London, "The Electromagnetic Equations of the Supraconductor", Reprinted from Proc. Roy. Soc., Vol. A149, pp. 71-88, [1935]
[2] Sewell, "Superconductivity", 8.14 Course Reader, [2007]
[3] J. Bardeen, L. N. Cooper, and J. R. Schrieffer, "Theory of Superconductivity", Physical Review, Vol. 108, No. 5, pp. 1175-1204, [1957]
[4] R. P. Feynman, Feynman Lectures on Physics, (Reading, MA, Addison-Wesley, 1965), "A Seminar on Superconductivity", Vol III, Chap. 21. [1965]
[5] Lakeshore Spec Sheet for DT-470 and DT-471 Silicon Diodes. [1986]
[6] Bedford, R.E. "Techniques for Approximating International Temperature Scale of 1990". Chapter 11. [1990]
[7] AZoM. "Critical Temperatures of some Type I Superconductors". The AZo Journal of Materials Online. www.azom.com [2008]
[8] Kittel, Charles and Kroemer, Herbert, Thermal Physics, 2nd Ed., W. H. Freeman, (via hyperphysics.phy-astr.gsu.edu. [1980]
[9] superconductors.org. "Type 2 Superconductors". Compiled data from NIST, CRC Handbook of Chemistry and physics, etc. [2008]
[10] Giaever, I. "Electron Tunneling Between Two Superconductors". Phys. Rev. Lett. 5, 464 - 466 [1960]
[11] Brewer, Jess H. "Measurement of the Temperature Dependence...". http://musr.org/theses/Sonier/MSc/thesis.html [2001]
[12] Bruynseraede, Y., Vlekken, C., and Van Haesendonck, C., "Giaever and Josephson Tunneling", NATO ASI Series, Vol. F59, Superconducting Electronics, Springer-Verlag [1989]

Acknowledgments

All non-linear fits were made with the MATLAB scripts made available to us on the Junior Lab website: http://web.mit.edu/8.13/www/jlmatlab.shtml.

We would like to thank the Junior Lab staff for the great year! Yeah!